Journal of Engineering Science and Technology
Vol. 15, No. 6 (2020) 4356 – 4366

GREEN SYNTHESIZED FE_2O_3 NANOPARTICLES AND IMMOBILIZATION ONTO BIOGENIC SILICA AS PHOTOCATALYST FOR PHOTO-DECOLORIZATION OF BROMOPHENOL BLUE

HESTI MEKARSARI[1], AGUS TAFTAZANI[1], AZLAN KAMARI[2], IS FATIMAH[1,*]

[1]Department of Chemistry, Faculty of Mathematics and Natural Sciences, Universitas Islam Indonesia, Kampus Terpadu UII, Jl. Kaliurang Km 14, Sleman, Yogyakarta, Indonesia
[2]Chemistry Department, Universiti Pendidikan Sultan Idris Perak, Perak 35900, Malaysia
*Corresponding Author: isfatimah@uii.ac.id

Abstract

Green synthesis of Fe_2O_3 nanoparticles and its immobilization onto biogenic silica nanocomposite (Fe_2O_3 NPs/SiO_2) for photocatalysis application have been conducted. Research is aimed to preserve low cost and high active photocatalyst material for dye degradation. Magnetite nanoparticles was synthesized using reduction method of Fe (III) precursor using *parkia speciossa hassk* (stinky bean) skin extract, meanwhile biogenic silica was extracted from bamboo leaves ash with the method as reported in previous studies. The nanocomposite was characterized by using x-ray diffraction, Fourier-transform infra-red, scanning electron microscope-energy dispersive x-ray, transmission electron microscope, and diffuses reflectance UV-visible spectroscopy. The photoactivity of the material was evaluated in bromo phenol blue decolorization via photocatalytic oxidation. Based on XRD and TEM analysis results, the nanocomposite contained nanosize Fe_2O_3 ranging at 10-100 nm with the mean of 48 nm. The nanocomposite demonstrated an excellent photo-decolorization of bromo phenol blue as shown by the degradation efficiency of about 98% for an hour treatment. The photocatalytic activity is in line with the band gap energy value of 2.4 eV as identified by UV-DRS analysis.

Keywords: Biogenic silica, Decolorization, Magnetite, Photocatalyst.

1. Introduction

Photocatalytic process for environmental application includes photocatalytic degradation of pollutant-contaminated water and air such as volatile organic compounds and dyes is an attracting process. The process is depending on the effectivity of photocatalyst materials. Refer to the green chemistry perspective, the advancement of photocatalyst materials is developed. Beside of good photoactivity, chemically inert, and suitability for absorbing visible or near UV light, reusability is also the main properties for a photocatalyst in the application scale. For that purposes the formation of photocatalyst in nanoparticles and supported form are widely developed [1]. Based on the quantum size effect theory, the nanosize form of semiconductor photocatalyst has higher activity because of localized surface plasmon resonance (LSPR) and interband transition effect [1, 2]. Several nanoparticles are reported to be active for photocatalytic degradation of dye such as magnetite nanoparticles, silver nanoparticles, SnO_2 nanoparticles, and Fe_2O_3 nanoparticles [2, 3].

Among these nanoparticles, Fe_2O_3 nanoparticles (furthermore called as Fe_2O_3 NPs) are characterized as economist, low band gap energy, and stability in aqueous medium. As another technique of nanoparticle synthesis, green approach for the synthesis of Fe_2O_3 NPs is widely studied by the use of eco-friendly agent, such as the use of plant extract [3]. Previous works reported the use of *Gardeniaresinifera* [4], *Rhus punjabensis* (Naz), *Glycosmis mauritiana* [5] plant extract as effective agent for iron oxide nanoparticles with size ranging from 30 to100 nm. Malarkodi et al. [6] reported the effectivity of green synthesized Fe_2O_3 NPs demonstrated photocatalytic activity for rhodamine 6G under visible light.

However, the use of nanoparticles in photocatalytic degradation of such organic pollutant has limitation related with rapid photoactivity loss caused by the presence of substrate that absorbs light and deteriorate its distribution, the loss of movement of particles. Immobilization of nanoparticles into a stable solid support is one technique that can be chosen to overcome this problem [4, 5]. Refer to the previous works, silica is a potential and easy to provide support for iron oxide nanoparticles, and based on renewable resource, the use biogenic silica is challenging [6]. Previous studies reported the use of biogenic silica from bamboo leaves ash as support for ZrO_2 and iron oxide via sol-gel reaction with that oxide precursors revealed the potency of biogenic silica combination for enhancing catalytic activity [7]. In another perspective of the development of nanoparticles photocatalysis with increasing activity, the combination of nanoparticles photocatalysis with its nanocomposite formation will be a novel material.

Considering previous works on the utilization of *parkia speciossa Hassk* extract (PSE) for green synthesis and the biogenic silica from bamboo leaves ash, this research interested to synthesize Fe_2O_3 NPs by using PSE and its immobilization onto biogenic silica from bamboo leaves [7, 8]. To our knowledge, the nanocomposite formation by combination of biogenic silica with green synthesized nanoparticles and its application for photocatalysis application has not been reported yet. Study on physicochemical properties and their impact to the photocatalytic activity will be an important aspect for further industrial applications. Research is aimed to evaluate the physicochemical properties of immobilized Fe_2O_3 NPs and photocatalytic activity for bromo phenol blue (BPB) degradation.

2. Materials and Method

2.1. Materials

Parkia speciossa Hassk was collected from Sleman district, Yogyakarta, Indonesia. Bamboo leaves ash was prepared by ashing dry leaves at 600°C for 2 h. Chemicals consist of $FeCl_3$, $FeSO_4.2H_2O$, NH_4OH, bromo phenol blue (BPB) were purchased from Merk-Millipore (Germany). PSE sample was prepared by boiling about 10 g small dry pieces of *Parkia speciossa Hassk* pod with 200 mL of water, followed by filtering using Whatman 41 paper.

2.2. Preparation of Fe_2O_3 NPs/SiO_2

Silica gel (SiO_2) was extraction from bamboo leave ash (BLA) was conducted referred to previous work reported [7]. SiO_2 was obtained by refluxing BLA in NaOH 4 M for 4 h followed by slow titration using HCl 0.2 N until gel formation (pH 8), and the gel was washed by aquadest.

Immobilization of Fe_2O_3 NPs into SiO_2 to form Fe_2O_3 NPs/SiO_2 nanocomposite was performed by mixing 100 mL of $FeCl_2.4H_2O$: $FeCl_3$.6H2O (0.1M:0.2M) with 25 mL of PSE. Into the mixture, 10mL of NaOH 0.1M solution was added. Theoretical Fe content in the composite was set up at 30 % wt. The mixture was ultrasound-mixed for 1 h followed by hydrothermal aging using autoclave at 100ºC overnight. The mixture was dried, and the obtained powder is Fe_2O_3 NPs/SiO_2. Physical characterization techniques were conducted by X-ray diffraction (XRD), Fourier Transformed Infrared Spectroscopy (FTIR), scanning electron microscope-energy dispersive x-ray (SEM-EDX), and diffuse reflectance UV-Visible spectroscopy (UV-DRS). XRD analysis was carried using X-ray diffractometer (Shimadzu X6000) with irradiation of Ni-filtered Cu Kα ($\lambda = 1.5406$ A°). FTIR analysis for was carried out over the spectral range of 400-4000 cm-1 on Perkin-Elmer. Phenom-X instrument was employed for SEM-EDX analysis, and for (UV-DRS) analysis, JASCO V760 instrument was utilized. The sample was analysed by using $BaSO_4$ as reference material.

2.3. Photocatalytic activity test

The photocatalytic activity of Fe_2O_3 NP/SiO_2 to the degradation of BPB using the photocatalytic reactor equipped with UV lamp 254 nm, 25 watt as described in Fig. 1. For each test, 20 mg of Fe_2O_3 NP/SiO_2 added into 500 mL of BPB solution 20 mg/L. The mixture was stirred under UV light exposure for the duration up to 60 min at the room temperature and neutral pH (pH =7). The sampling was conducted by taking 3 mL of treated solution at the 15 min interval time. Each sample was settled before analysis using UV-Vis spectrophotometric analysis. A HITACHI U 2010 spectrophotometer was utilized for the analysis.

Degradation efficiency (DE) was calculated based on concentration at initial and at 60 min using following equation:

$$DE\ (\%) = 100\ x\ \frac{C_0 - C_t}{C_0} \quad (1)$$

where C_o is the initial concentration of BPB, and C_t is the concentration of BPB at 60 min.

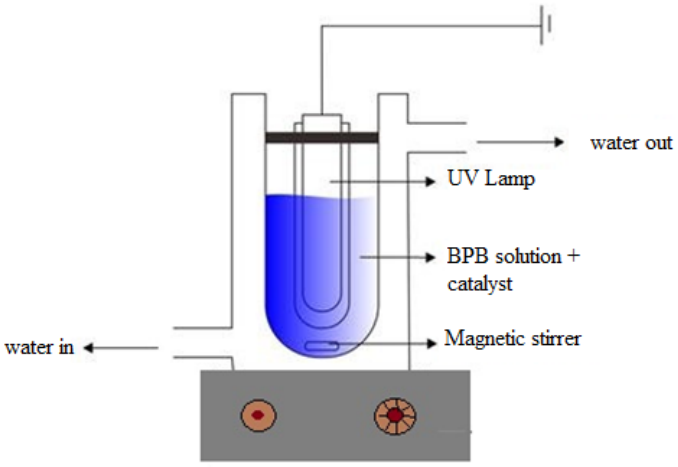

Fig. 1. Scheme of photocatalytic reactor.

3. Results and Discussion

3.1. Physicochemical character of material

XRD pattern of Fe_2O_3 NPs/SiO_2 compared with SiO_2 which extracted from BLA (Fig. 2). The reflection of SiO_2 shows the amorphous silica as identified by broad-spectrum at 25°. Moreover, Fe_2O_3 NP/SiO_2 reveals that the material conform the presence of Fe_2O_3 nanoparticles as determined by some reflections at 24.16, 33.12, 35.63, 40.64, 9.47, 54.08 and 57.42 which be attributed to the 012, 104, 110,113, 024, 116 and 018 crystalline structures corresponding to α-Fe_2O_3 nanoparticles refer to JCPDS File No. 86-0550 [8, 9].

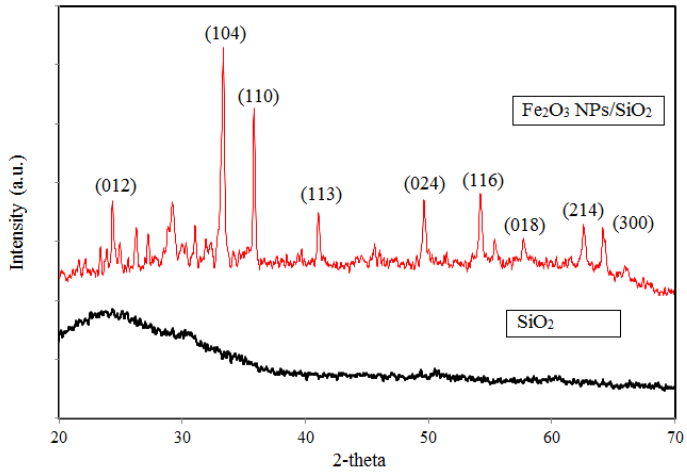

Fig. 2. XRD pattern of SiO_2 and Fe_2O_3 NPs/SiO_2.

The crystallite size of dispersed Fe_2O_3 NP was calculated by using Scherrer's formula, Eq. (2):

$$D = \frac{K\lambda}{\beta.cos\theta} D \quad (2)$$

where, K is 0.9, λ is wavelength of x-ray source (0.154068 nm), β is full width at half maximum in radians, and θ is Bragg's diffraction angle [10]. From all significant peaks, the calculated crystallite size is ranging from 42.7 - 54.0 nm. This range of crystallite size is more homogeneous and smaller compared with Fe_2O_3 synthesized by precipitation method [9] and Fe_2O_3 synthesized using *Acacia nilotica* pods extract [11].

Effect of Fe_2O_3 immobilization onto SiO_2 is confirmed by the change in surface profile from SEM profile (Fig. 3). The rougher cubic-like aggregates appear in Fe_2O_3 NPs/SiO_2 relative to SiO_2 suggesting the deposited iron oxide nanoparticles in the composite [4]. The profile is similar with the immobilized iron oxide onto silica from bamboo leave by precipitation method [7, 12]. The EDX analysis results presented in Table 1 suggest that the Fe content in the Fe_2O_3 NPs/SiO_2 is about 31.2 %wt., slightly higher than the set up theoretical Fe content of 30 %wt. This referred to the weight loss of the support caused by the calcination process.

Table 1. EDX analysis result.

Component	Content (% wt.)	
	SiO_2	**Fe_2O_3 NPs/SiO_2**
Fe	Not detected	31.2
Si	45.78	26.2
O	54.22	42.6

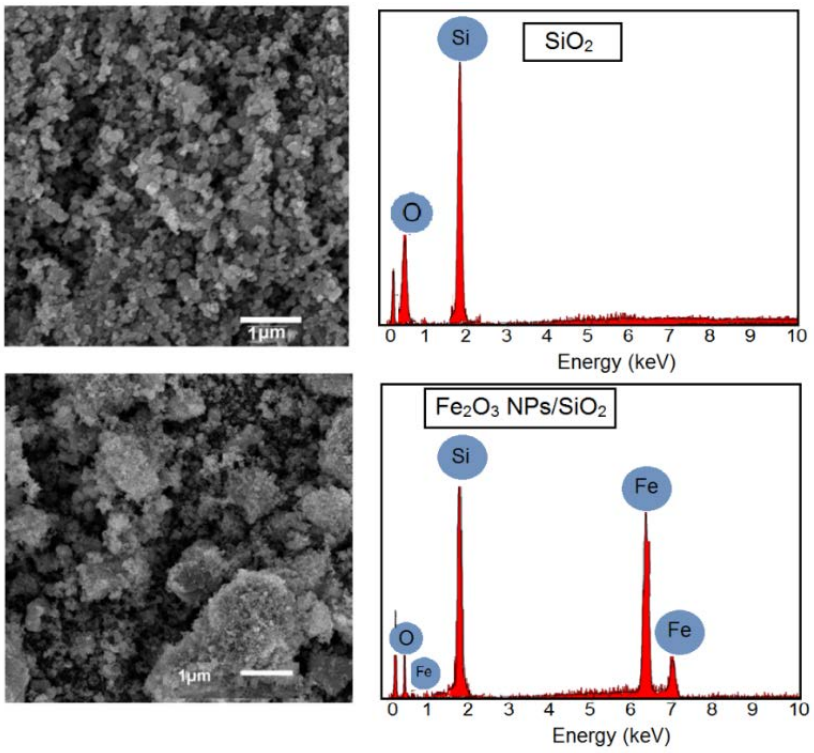

Fig. 3. SEM profile of SiO_2 and Fe_2O_3 NPs/SiO_2.

To make clear representation of dispersed nanoparticle onto silica in the nanocomposite, TEM analysis was performed, and the image is presented in Fig. 4. The Fe_2O_3 NPs/SiO_2 image shows the irregular spherical nanoparticles with the size ranging at 30-60 nm deposited onto silica support, with the mean diameter of 52 nm. The structure represents the core-shell structure which Fe_2O_3 NPs appear as a core within the silica shell as clear depicted by the figure in the inset. This result is similar with the green synthesized Fe_2O_3@SiO_2 reported by previous works [13, 14], suggesting that the sol-gel coating was occurred during the dispersion of Fe_2O_3 NPs onto silica support, and in addition, this implies chemical interaction between iron and silica [15]. The particle size obtained from the TEM analysis is in line with crystallite size ranging from 42.7 - 54.0 obtained by XRD measurement.

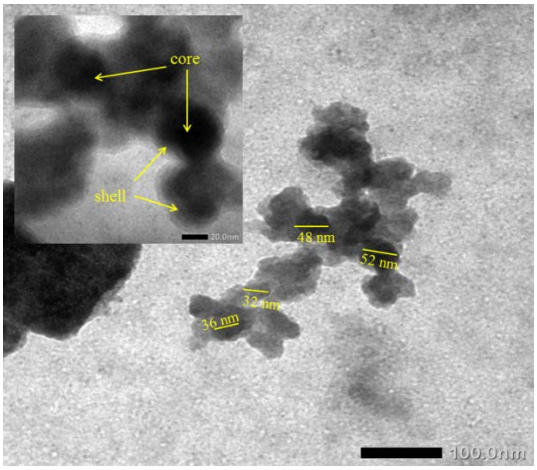

Fig. 4. TEM profile of Fe_2O_3 NPs/SiO_2.

Furthermore, the occurring interaction between Fe and Si in the composite as represented by TEM analysis is identified by FTIR analysis (Fig. 5).

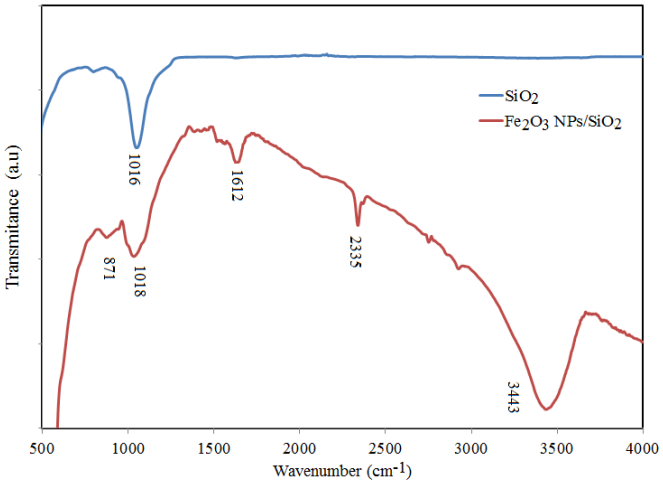

Fig. 5. FTIR spectra of SiO_2 and Fe_2O_3 NPs/SiO_2.

Both materials show the strong and sharp peak at 1016 cm^{-1} which attributed to the asymmetric stretching vibration of SiO_2 bonds. The presence of Fe-O-Si interaction is revealed by the peak at 871 cm^{-1}. The peak at 1612 cm^{-1} and 2335 cm^{-1} in Fe_2O_3 NP/SiO_2 are assigned to the presence of OH and C-H that are probably coming from the PSE, respectively.

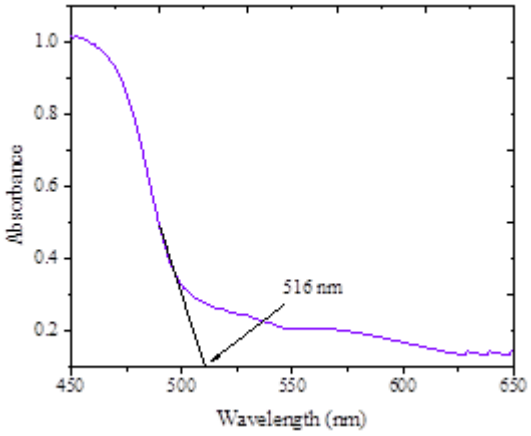

Fig. 6. UV-DRS spectrum of Fe_2O_3 NPs/SiO_2.

As photocatalyst, the band gap energy is an important parameter determining the capability of nanomaterial to catch light for further oxidation mechanism. Diffuse reflectance UV-Vis (UV-DRS) analysis was performed to determine the band gap energy of nanocomposite, and the spectrum is presented in Fig. 6. The spectrum demonstrates the absorption bands dominantly the ultraviolet region (200-400 nm) and less absorbance at visible region. The band at UV region is related to the ligand-to-metal charge transfer (290-390 nm), while at visible region (400-600 nm) is assigned to the pair excitation processes and surface plasmon resonance of the nanoparticle. The nanocomposite shows the edge wavelength at 516 nm which coincides with the band gap energy of 2.4 eV.

3.2. Photocatalytic activity of material

Figures 7(a) and (b) show the time evolution of the UV-Vis spectra of BPB solution under the photocatalytic degradation treatments with and without H_2O_2 addition. BPB solution expresses the maximum wavelength at about 594 nm. From both spectra, it is confirmed that the treated solutions depict the reduced and even loss absorbance of the maximum wavelength. Under both treatments, it is seen that the absorbance values are reduced along with the increasing time of treatment. Based on these reduced values, the kinetics plot of both treatments is depicted in Fig. 7(c). By comparing both patterns, the treatment using H_2O_2 demonstrates the faster degradation rate compared to the treatment without H_2O_2.

This higher degradation rate refers to the more oxidant produced from the interaction between •OH released by the photon-Fe_2O_3 surface interaction [13, 16]. As the photon from UV lamp impinged the surface of semiconductor in the solution, the electron at the valence band of Fe_2O_3 is excited into the conductance band and leave hole h+. Furthermore, the •OH will be formed after the interaction

between h+ with -OH from solvent. Propagation steps to establish more oxidant are refers to following mechanism:

$$Fe_2O_3 + hv \rightarrow e^-_{CB} + h^+_{VB}$$
$$h^+_{VB} + OH^-_{(Fe2O3\ surface)} \rightarrow \bullet OH$$
$$h^+_{VB} + H_2O_{(adsorbed\ on\ surface)} \rightarrow \bullet OH + H^+$$
$$\bullet OH + O_2 \rightarrow \bullet OOH$$
$$e^- + O_2 \rightarrow O_2^-$$
$$O_2 + H^+ \rightarrow \bullet OOH$$
$$\bullet OOH + \bullet OH + BPB \rightarrow \text{degradation product} + CO_2 + H_2O + Br^-$$

In order to evaluate the kinetics aspect of the reactions, pseudo-first-order and pseudo-second-order kinetics models were applied by the following equations [17]:

$$ln\frac{C_0}{C_t} = k_1 \quad (3)$$
$$\frac{1}{C_t} = k_2 t + \frac{1}{C_0} \quad (4)$$

with C_o and C_t were the initial concentration of BPB and concentration at t time, respectively, and k_1 and k_2 were kinetics constant for pseudo-first order and pseudo-second-order model, respectively. The parameter of the models and the degradation efficiency data are presented in Table 2.

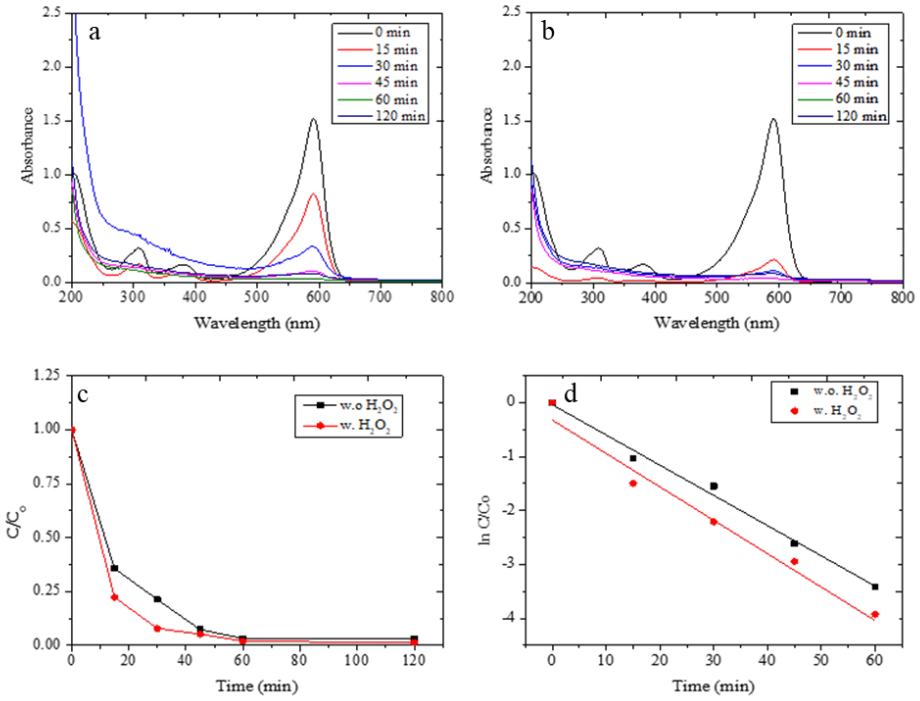

Fig. 7. (a) UV-visible spectra of treated solution without H_2O_2 (b) UV visible spectra of treated solution with H_2O_2 (c) Kinetics plot of BPB degradation (d) Pseudo-first-order plot of BPB degradation.

Table 2. Kinetics parameter of photocatalytic degradation of BPB with and without H_2O_2 at room temperature.

Reaction	R^2 of Pseudo-first order model	R^2 of Pseudo-second order	Kinetics equation	*k* (L/mg.min)	*DE* (%)
Without H_2O_2	-0.9913	0.9011	$ln\ C = -0.062\ t - 0.257$	0.067	98.01
With H_2O_2	-0.9858	0.8518	$ln\ C = -0.105\ t - 0.038$	0.105	99.89

The R^2 parameters imply that the kinetics of photocatalytic degradation obeys pseudo-first-order model (Fig. 7(d)). This fitness is generally accepted for photocatalytic-dye degradation including BPB photodegradation over such as iron oxide photocatalysts [18-21]. The *DE* values from these experiments are relatively high compared with similar research utilizing various photocatalyst as presented in Table 3.

Table 3. DE values of BPB photocatalytic degradation using various photocatalysts.

Photocatalyst	*DE* (%)	Remark	Reference
Magnetic Fe_3O_4	94	*Cynometra ramiflora* fruit extract	[18]
Chitosan-conjugated magnetic	94.5	The highest DE is 94.5	[21]
$Fe/ZnO/SiO_2$	100	DE was evaluated by 30 min of treatment	[22]
TiO_2 nanoparticles	85.51	DE was evaluated by 200 min of treatment	[23]
AgBr-ZnO	89.3	DE was evaluated by 50 min of treatment, using H_2O_2 addition	[24]
Fe_2O_3 NPs/SiO_2	99.89	DE was evaluated by 60 min of treatment, using H_2O_2 addition	This research

4. Conclusion

Fe_2O_3 NPs/SiO_2 was successfully prepared by dispersing Fe_2O_3 NPs synthesized using *parkia speciossa Haskk* extract by into SiO_2 extracted from bamboo leaves ash. The physicochemical characterization of the composite showed the formation of crystalline Fe_2O_3 NPs dispersed onto SiO_2 with the particle size ranging from 30-60 nm. The composite exhibits the photocatalytic activity towards the BPB degradation as shown by kinetics plot which obey pseudo-first order kinetics. It is noted that the addition of H_2O_2 into the photocatalytic system improves degradation efficiency from 98.01 without H_2O_2 to 99.89 % with H_2O_2. The degradation efficiency values suggest the potency of the nanocomposite to be applied in the photocatalytic treatment of dye-containing wastewater.

Nomenclatures

C_o	Initial concentration
D	Crystallite size
DE	Degradation efficiency
k	Kinetics constant
K	Diffraction factor
R^2	Determination coefficient

Greek Symbols

θ	Diffraction angle
λ	Wavelength

Abbreviations

BPB	Bromophenol blue
JCPDS	Joint Committee of Pure Diffraction Spectra
PSE	Parkia Speciossa Extract

References

1. Fierascu, R.C.; Ortan, A.; and Avramescu, S.M.; and Fierascu, I. (2019). Phyto-nanocatalysts: green synthesis, characterization, and applications. *Molecule*, 24(19), 1-35.
2. Leong K.H.; Aziz, A.A.; Sim, L.C.; Saravanan, P.; Jang, M.; and Bahnemann, D. (2018). Mechanistic insights into plasmonic photocatalysts in utilizing visible light. *Beilstein Journal of Nanotechnology*, 9, 628-648.
3. Fahmy, H.M.; Mohamed, F.M.; Marzouq, M.H.; Mustafa, A.B.E.; Alsoudi, A.M.; Ali, O.A.; Mohamed, M.A.; and Mahmoud, F.A. (2018). Review of green methods of iron nanoparticles synthesis and applications. *BioNanoScience*, 8, 491-503.
4. Ali, A.; Zafar, H.; Zia, M.; Haq, I.U.; Phull, A.R.; Ali, J.S.; and Hussain, A. (2016). Synthesis, characterization, applications, and challenges of iron oxide nanoparticles. *Nanotechnology, Science and Applications*, 9, 49-67.
5. Moghaddam, M.M.; Pieber, B.; Glasnov, T.; and Kappe, C.O. (2014). Immobilized iron oxide nanoparticles as stable and reusable catalysts for hydrazine-mediated nitro reductions in continuous flow. *ChemSusChem*, 7(11), 3122-3131.
6. Sharafi, Z.; Bakhshi, B.; Javidi, J.; and Adrangi, S. (2018). Synthesis of silica-coated iron oxide nanoparticles: preventing aggregation without using additives or seed pretreatment. *Iranian Journal of Pharmaceutical Research*, 17(1), 386-395.
7. Fatimah, I.; Amaliah, S.N.; Andrian, M.F.; Handayani, T.P.; Nurillahi, R.; Prakoso, N.I.; Wicaksono, W.P.; and Chuenchom, L. (2019). Iron oxide nanoparticles supported on biogenic silica derived from bamboo leaf ash for rhodamine B photodegradation. *Sustainable Chemistry and Pharmacy*, 13.
8. Khalil, A.T.; Ovais, M.; Ullah, I.; Ali, M.; Shinwari, Z.K.; and Maaza, M. (2017). Biosynthesis of iron oxide (Fe_2O_3) nanoparticles via aqueous extracts of *Sageretia thea* (Osbeck.) and their pharmacognostic properties. *Green Chemistry Letters and Reviews*, 10(4), 186-201.

9. Lassoued, A.; Dkhil, B.; Gadri, A.; and Ammar, S. (2017). Control of the shape and size of iron oxide (α-Fe_2O_3) nanoparticles synthesized through the chemical precipitation method. *Results in Physics*, 7, 3007-3015.
10. Dong, C.; Chen, C.; and Hung, C. (2017). Synthesis of magnetic biochar from bamboo biomass to activate persulfate for the removal of polycyclic aromatic hydrocarbons in marine sediments. *Bioresource Technology*, 245(Part A), 188-195.
11. Da'na, E.; Taha, A.; and Afkar, E. (2018). Green synthesis of iron nanoparticles by Acacia *nilotica* pods extract and its catalytic, adsorption, and antibacterial activities. *Applied Sciences*, 8(10), 1922-1934.
12. Fatimah, I.; Taushiyah, A.; Najah, F.B.; and Azmi, U. (2018). ZrO_2/bamboo leaves ash (BLA) catalyst in biodiesel conversion of rice bran oil. *IOP Conference Series: Materials Science and Engineering*, 349.
13. Mortazavi-Derazkola, S.; Salavati-Niasari, M.; Khojasteh, H.; Amiri, O.; and Ghoreishi, S.M. (2017). Green synthesis of magnetic Fe_3O_4/SiO_2/HAp nanocomposite for atenolol delivery and in vivo toxicity study. *Journal of Cleaner Production*, 168, 39-50.
14. Obaidullah, M.; Bahadur, N.M.; Furusawa, T.; Sato, M.; Sakuma, H.; and Suzuki, N. (2019). Microwave assisted rapid synthesis of Fe_2O_3@SiO_2 core-shell nanocomposite for the persistence of magnetic property at high temperature. *Colloids and Surfaces A: Physicochemical and Engineering Aspects*, 572, 138-146.
15. Munasir, A.S.; Dewanto, A.S.; Kusumawati, D.H.; Putri, N.P.; Yulianingsih, A.; Sa'adah, I.K.F.; Taufiq, A.; Hidayat, N.; Sunaryono, S.; and Supardi, Z.A.I. (2018). Structure analysis of Fe3O4@SiO_2 core shells prepared from amorphous and crystalline SiO_2 particles. *IOP Conference Series: Materials Science and Engineering*, 367.
16. Dlamini, L.N.; Krause, R.W.; Kulkarni, G.U.; and Durbach, S.H. (2011). Photodegradation of bromophenol blue with fluorinated TiO_2 composite. *Applied Water Science*, 1, 19-24.
17. Bishnoi, S.; Kumar, A.; and Selvaraj, R. (2018). Facile synthesis of magnetic iron oxide nanoparticles using inedible *Cynometra ramiflora* fruit extract waste and their photocatalytic degradation of methylene blue dye. *Materials Research Bulletin*, 97, 121-127.
18. Pereira, M.C.; Oliveira, L.C.A.; and Murad, E. (2012). Iron oxide catalysts: fenton and fenton-like reactions - a review. *Clay Minerals*, 47, 285-302.
19. Mishra, M.; and Chun, D. (2015). α-Fe_2O_3 as a photocatalytic material: a review. *Applied Catalysis A: General*, 498, 126-141.
20. Khan, H.; Khalil, A.K.; Khan, A.; Saeed, K.; and Ali, N. (2016). Photocatalytic degradation of bromophenol blue in aqueous medium using chitosan conjugated magnetic nanoparticles. *Korean Journal of Chemical Engineering*, 33, 2802-2807.
21. Mohamed, R.M.; Mkhalid, I.A.; Baeissa, E.S.; and Al-Rayyani, M.A. (2012). Photocatalytic degradation of methylene blue by Fe/ZnO/SiO_2 nanoparticles under visible light. *Journal of Nanotechnology*, Article ID 329082.